

## STATUS OF PETC's METHANE-TO-HIGHER HYDROCARBON PROCESS

Charles E. Taylor, Richard P. Noceti, Curt M. White,  
Mark A. McDonald, Richard R. Anderson, Donald V. Martello

U.S. Department of Energy  
Pittsburgh Energy Technology Center  
P.O. Box 10940  
Pittsburgh, PA 15236-0940  
412-892-6058

### ABSTRACT

Research at the Pittsburgh Energy Technology Center has led to a two-stage process for the conversion of methane to gasoline-range hydrocarbons<sup>1,2</sup>. Methane, oxygen, and hydrogen chloride react over an oxyhydrochlorination (OHC) catalyst in the first stage to produce predominately chloromethane and water. In the second stage, the chloromethane is catalytically converted to higher hydrocarbons, mainly in the gasoline (C<sub>4</sub>-C<sub>10</sub>) boiling range, by a pentasil-type zeolite such as ZSM-5. Earlier studies exhibit conversions of typically 40% for the conversion of methane to chloromethane and 98+% for the conversion of chloromethane to higher hydrocarbons.

The first stage reaction has been studied under varying conditions of temperature and feed stoichiometry and over a range of residence times. The conversion of reactants, the yields, and product selectivities have been determined over the operating range of the catalyst.

The second-stage reaction has been carried out over a zeolite catalyst with chloromethane and various mixtures of chloromethane, dichloromethane, and trichloromethane as reactants. The products of reaction were similar to those formed when using methanol as a feed. The catalyst has shown no significant changes in conversions or product distribution after multiple cycles of deactivation and oxidative regeneration.

### OBJECTIVE

The objective of this project is to obtain the scientific and engineering data necessary to design and operate an integrated PDU-scale system for the conversion of methane and other light hydrocarbons to liquid, gasoline-range hydrocarbons. This objective will be accomplished by splitting the project into four separate tasks:

- (1) Catalyst Preparation and Screening.
- (2) Activation of Methane Under Pressure.
- (3) Product Characterization.
- (4) Mechanism Studies.

Each of these tasks is conducted by a different principle investigation team and will be discussed separately.

## CATALYST PREPARATION AND SCREENING

This portion of the research involves the preparation, screening and development of the OHC catalysts. Techno-economic evaluations indicate that improvements in the first (OHC) stage will lead to more favorable overall process economics. In this light, several new OHC catalysts were synthesized and evaluated for activity.

## EXPERIMENTAL

The catalysts were prepared by sequential deposition of the appropriate metal chlorides, or their precursors, in non-aqueous solvents onto a fumed silica support. The catalysts were tested for OHC activity under a predetermined set of conditions and compared to the original copper catalyst. A blank was prepared under identical conditions to those used for the others except that no base metals were added. The catalysts were activated in a stream of hydrogen chloride at 300°C prior to testing. Composition of the catalysts, by weight, is given in Table I.

## RESULTS AND DISCUSSION

Table II lists reactant conversions under conditions utilized for the original copper catalyst and Table III lists the normalized carbon product distribution. With the exception of the cobalt catalyst, all exhibited a lower conversion of methane and lower chloromethane production than the copper catalyst. Temperature profiles of the catalysts were performed along with lifetime studies for the copper and cobalt catalysts. Reactant conversion and product distribution remained constant during the 400 hours on stream. The new catalysts exhibit a wide range of product distributions over the product slate.

Differences in activity of the OHC catalysts have been observed depending on who prepared them. These differences result in lower conversions and poorer selectivity for chloromethane. In an effort to understand why these differences occur, physical characterization of the catalysts is under investigation.

Preliminary scanning electron microscopic (SEM) examination of two (2) supported OHC catalyst samples showed some differences in morphology and segregation of Cu, Cl, La, and K. The overall elemental composition of the two samples are similar, as shown in the energy dispersive spectroscopy (EDS) spectra (Figures 1 & 2), however, the SEM micrographs display a difference in particle size. The more active catalyst exhibits a finer particle texture with fewer large copper-potassium chloride needles. Identical results were observed for a two samples of the Co-OHC catalyst which exhibited different OHC activities (Figures 3-6).

X-ray diffraction (XRD) performed on the two Cu-OHC catalyst samples utilizing a Cu-K $\alpha$  radiation exhibited some differences. The most significant was at 2 $\theta$  angles of 11.6 and 6.05 degrees. The more active catalyst exhibits intensities at these positions which are greater by a factor of 2 and 5 respectively. Upon exposure to air the 2 $\theta$  peak at 6.05 degrees disappears. Further research into the what this phase is and why it is susceptible to exposure to the atmosphere

is under investigation.

TABLE I CONSTITUENTS BY WEIGHT

CATALYST	% METAL CHLORIDE	%SiO <sub>2</sub>	%KCl	%LaCl <sub>3</sub>
Cu	41.66	37.50	11.46	9.38
Co	55.17	28.82	8.81	7.20
Ni	58.46	26.70	8.16	6.68
Pb	66.96	21.24	6.49	5.31
Ag	44.73	35.53	10.86	8.88
Pt	41.66	37.50	11.46	9.38
Cr	56.24	28.12	8.61	7.03
BLANK	0.00	64.29	19.64	16.07

TABLE II REACTANT CONVERSION

CATALYST	%CH <sub>4</sub> CONV	%HCl CONV	%O <sub>2</sub> CONV
Cu	47.69	80.08	83.86
Co	61.03	52.54	85.48
Ni	19.31	19.81	11.11
Pb	5.51	14.86	9.41
Ag	4.54	7.95	14.03
Pt <sup>a</sup>	54.34	0.01	3.10
Pt <sup>b</sup>	7.36	3.29	6.56
Cr	13.15	3.54	33.21
BLANK	16.16	6.63	25.31

3.0 GRAMS CATALYST, RESIDENCE TIME 8.3 SECONDS, TEMP. 340°C, FLOWS CH<sub>4</sub> = HCl = 4.0 mL/MIN, O<sub>2</sub> = N<sub>2</sub> = 2.0 mL/MIN

TABLE III NORMALIZED CARBON PRODUCT DISTRIBUTION

CATALYST	CH <sub>3</sub> Cl	CH <sub>2</sub> Cl <sub>2</sub>	CHCl <sub>3</sub>	CCl <sub>4</sub>	CO	CO <sub>2</sub>	HCOOH
Cu	30.03	39.42	9.39	0.14	0.00	12.44	8.58
Co	44.31	12.44	1.32	0.00	0.00	3.67	38.26
Ni	23.03	3.78	0.00	0.00	0.00	0.00	73.19
Pb	20.97	3.49	0.37	0.00	0.00	0.00	75.17
Ag	12.71	1.37	0.09	0.00	0.00	14.52	71.31
Pt <sup>a</sup>	31.26	3.49	0.30	0.18	0.00	17.35	47.42
Pt <sup>b</sup>	28.96	3.28	0.42	0.14	0.00	10.75	56.45
Cr	10.92	2.66	0.60	0.00	64.77	21.05	0.00
BLANK	10.10	0.45	0.09	0.00	69.55	7.02	12.78

3.0 GRAMS CATALYST, RESIDENCE TIME 8.3 SECONDS, TEMP. 340°C, FLOWS CH<sub>4</sub> = HCl = 4.0 mL/MIN, O<sub>2</sub> = N<sub>2</sub> = 2.0 mL/MIN

<sup>a</sup>After 24 hours on stream

<sup>b</sup>After 48 hours on stream

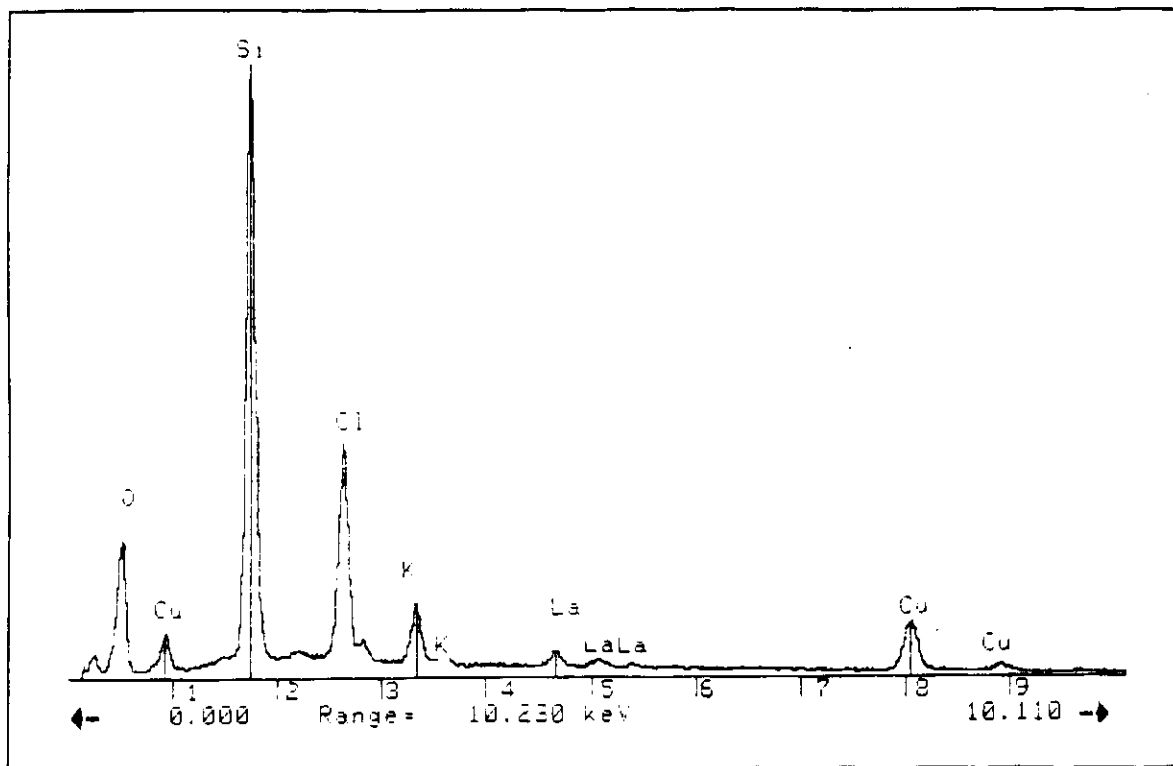


FIGURE 1. EDS SPECTRUM OF LOW ACTIVITY Cu-OHC CATALYST.

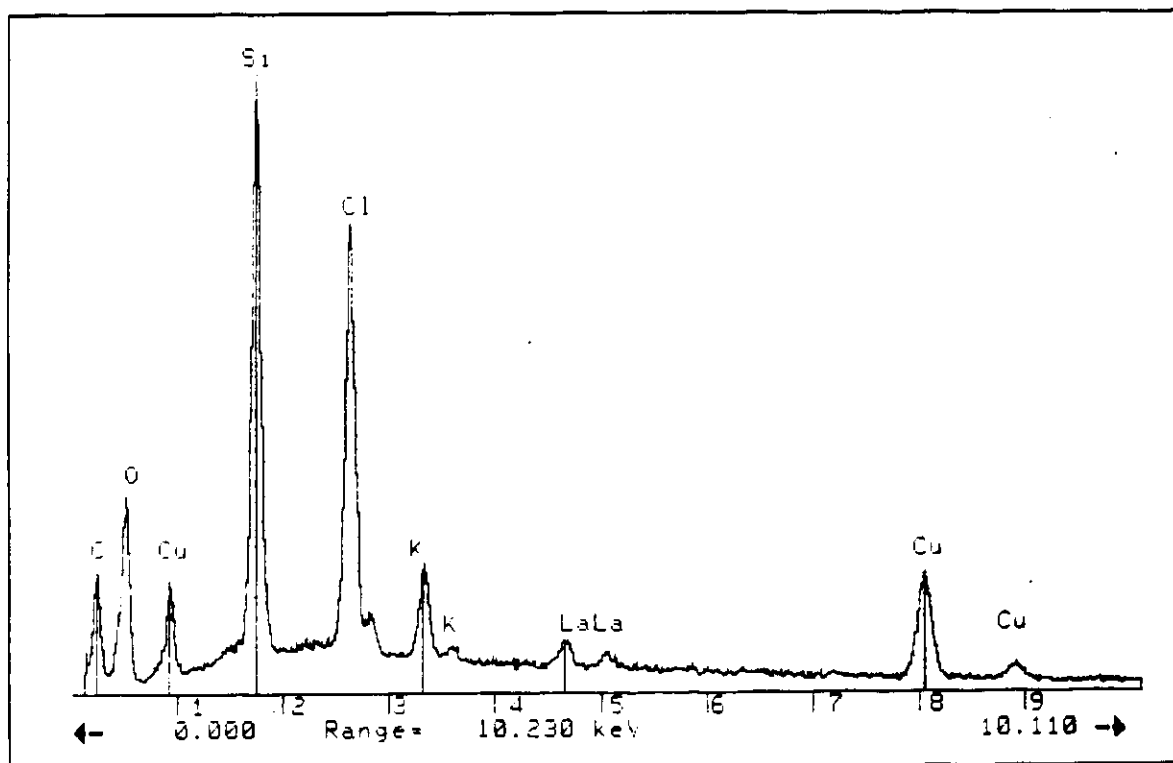


FIGURE 2. EDS SPECTRUM OF HIGH ACTIVITY Cu-OHC CATALYST.

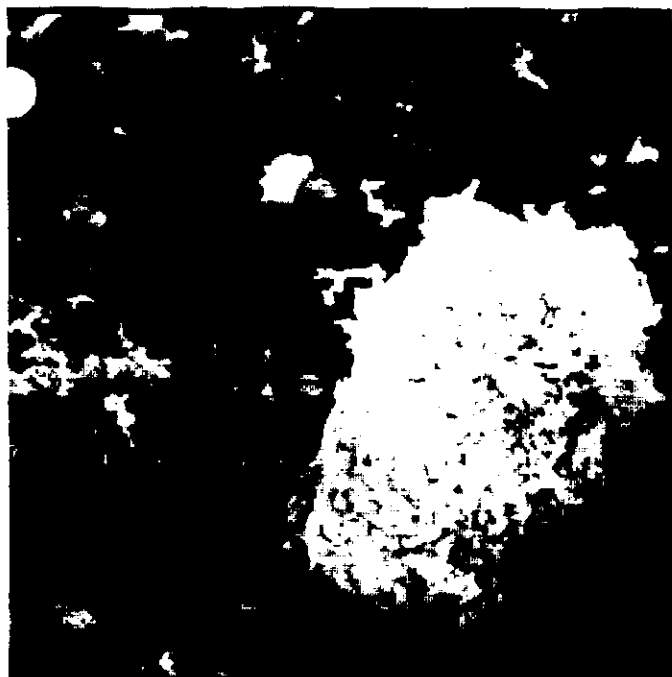


FIGURE 3. SEM OF HIGH ACTIVITY Co-OHC CATALYST, 500X.



FIGURE 4. SEM OF HIGH ACTIVITY Co-OHC CATALYST, 5000X.

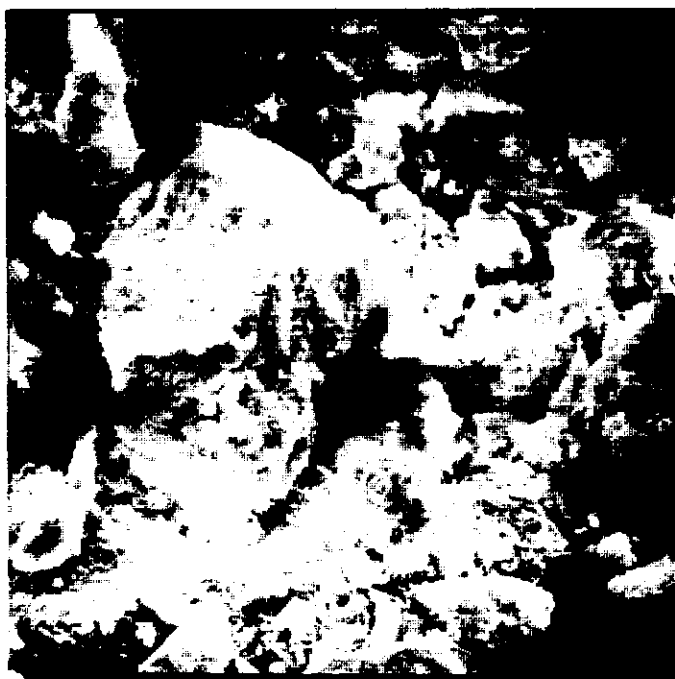


FIGURE 5. SEM OF LOW ACTIVITY Co-OHC CATALYST, 500X.

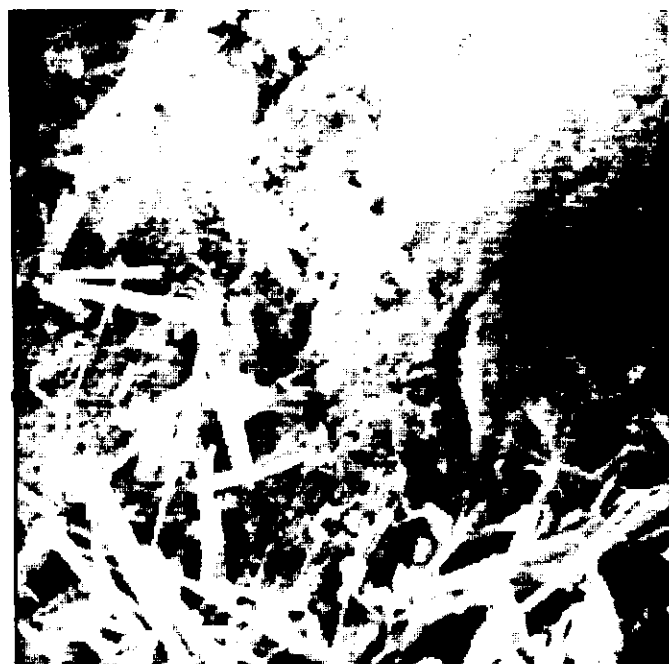


FIGURE 6. SEM OF LOW ACTIVITY Co-OHC CATALYST, 5000X.

# REACTANT CONVERSION OVER Cu-OHC CATALYST

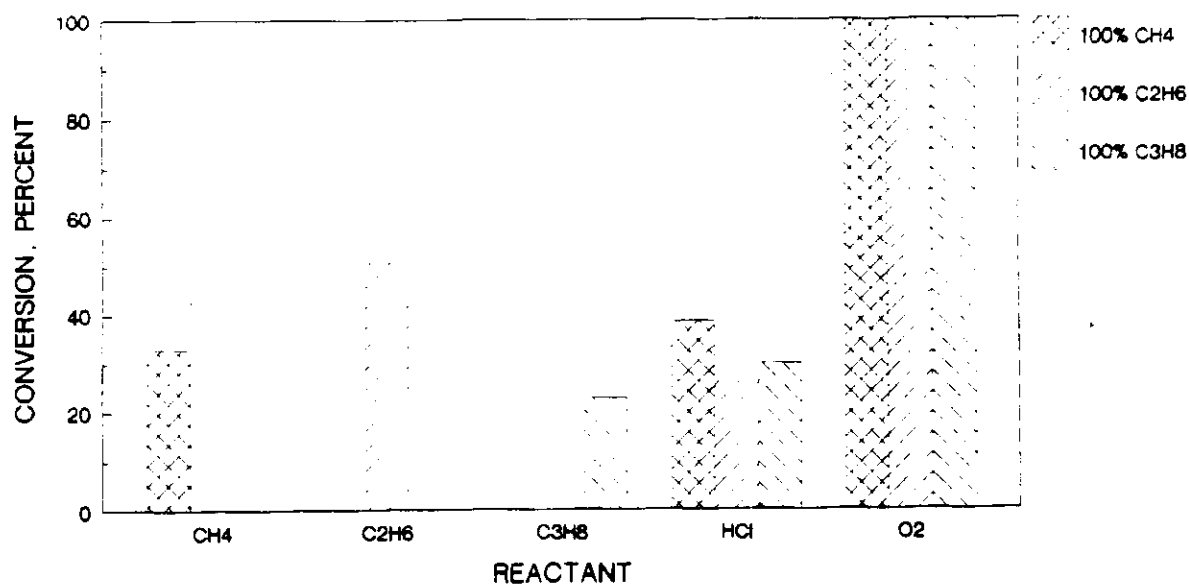


FIGURE 7. PLOT OF REACTANT CONVERSION FOR PURE HYDROCARBONS OVER Cu-OHC CATALYST.

# REACTANT CONVERSION OVER Cu-OHC CATALYST OF SYNTHETIC NATURAL GAS MIXTURE

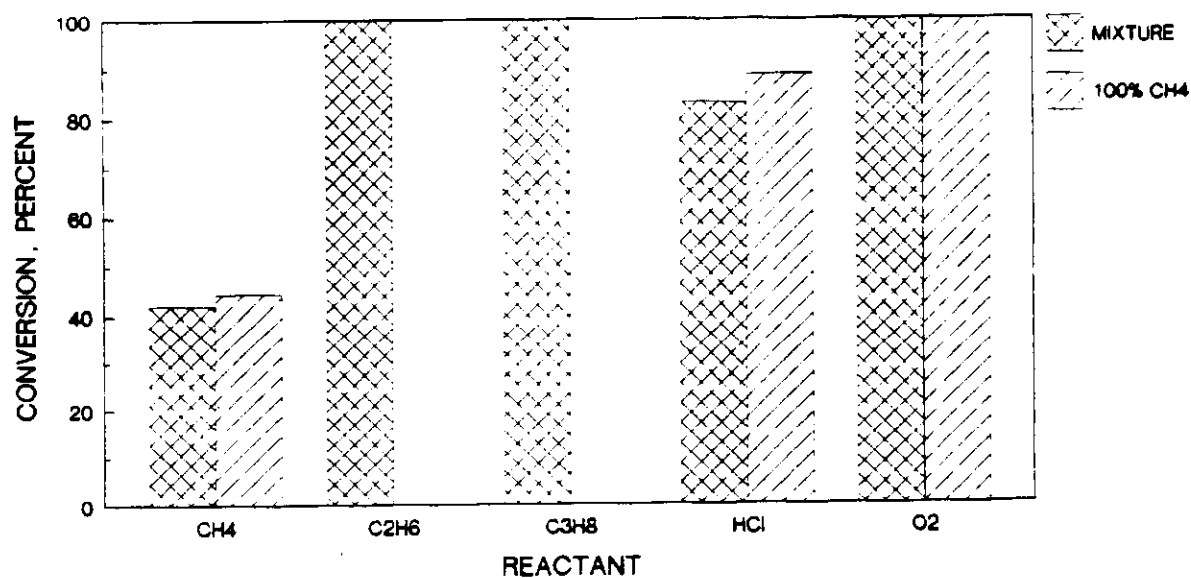


FIGURE 8. PLOT OF REACTANT CONVERSION FOR HYDROCARBON MIXTURE OVER Cu-OHC CATALYST.

## CONVERSION OF HIGHER HYDROCARBONS OVER Cu-OHC CATALYST

### EXPERIMENTAL

A mixture of 77.5 mole % methane, 15 mole % ethane, and 7.5 mole % propane along with pure ethane and propane were allowed to react over a Cu-OHC catalyst. The mixture was selected to simulate a natural gas feed to the first-stage reactor. Reaction conditions in each run were: HCl flow of 4.0 mL/min, O<sub>2</sub> and He flows of 2.0 mL/min, 3.0 grams freshly activated Cu-OHC catalyst and reaction temperature of 342°C.

### RESULTS

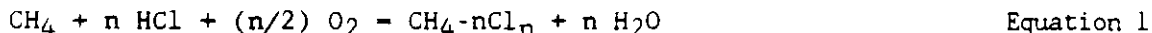
Figures 7 & 8 show the reactant conversion of the gas mixture and the pure components respectively. In the mixture conversion of ethane and propane were 100% while conversion of methane was approximately the same as that in the pure methane feed.

Further research to identify optimum operating conditions and product composition for conversion of the higher hydrocarbons over the Cu-OHC catalyst are currently under investigation.

### ACTIVATION OF METHANE UNDER PRESSURE

Economic analysis of the PETC process for direct methane conversion indicate that it can convert light hydrocarbon feeds into more valuable liquid fuels at a lower cost than any competing direct conversion process<sup>3</sup>. Although laboratory tests have shown that catalysts for each stage of the two-stage PETC process give good test has been made at the higher pressures typical for commercial application (100-300 psig). A central goal in the development of the PETC process is therefore to obtain reliable catalyst data at realistic industrial operating conditions.

In order to fill this gap in the catalyst database, a unit was constructed to test methane conversion catalysts at 150 psig total pressure. This unit (Figure 9) can test catalysts for the first-stage reaction, oxyhydrochlorination (OHC) of methane:



Promoted copper on high-surface-area fumed silica is currently the OHC catalyst utilized due to its good activity and selectivity in laboratory tests. The unit can also test catalysts for the second-stage reaction, oligomerization of chloromethanes to aromatics and light olefins. The unit has been constructed and shakedown is nearly complete. Low-pressure tests with the first-stage copper catalyst have reproduced laboratory data, and catalyst is currently being tested at higher pressure. The main variables in catalyst tests during the next year are temperature, space velocity, and %CH<sub>4</sub>, %HCl, and %O<sub>2</sub> in the feed, with total pressure typically held constant at 150 psig. From this data, it will be apparent what conditions give good conversions to CH<sub>3</sub>Cl without excessive amounts of polychlorinated methanes or oxidation products. At least one long-term continuous run will test catalyst life.

# High-Pressure Methane Conversion Flow Diagram

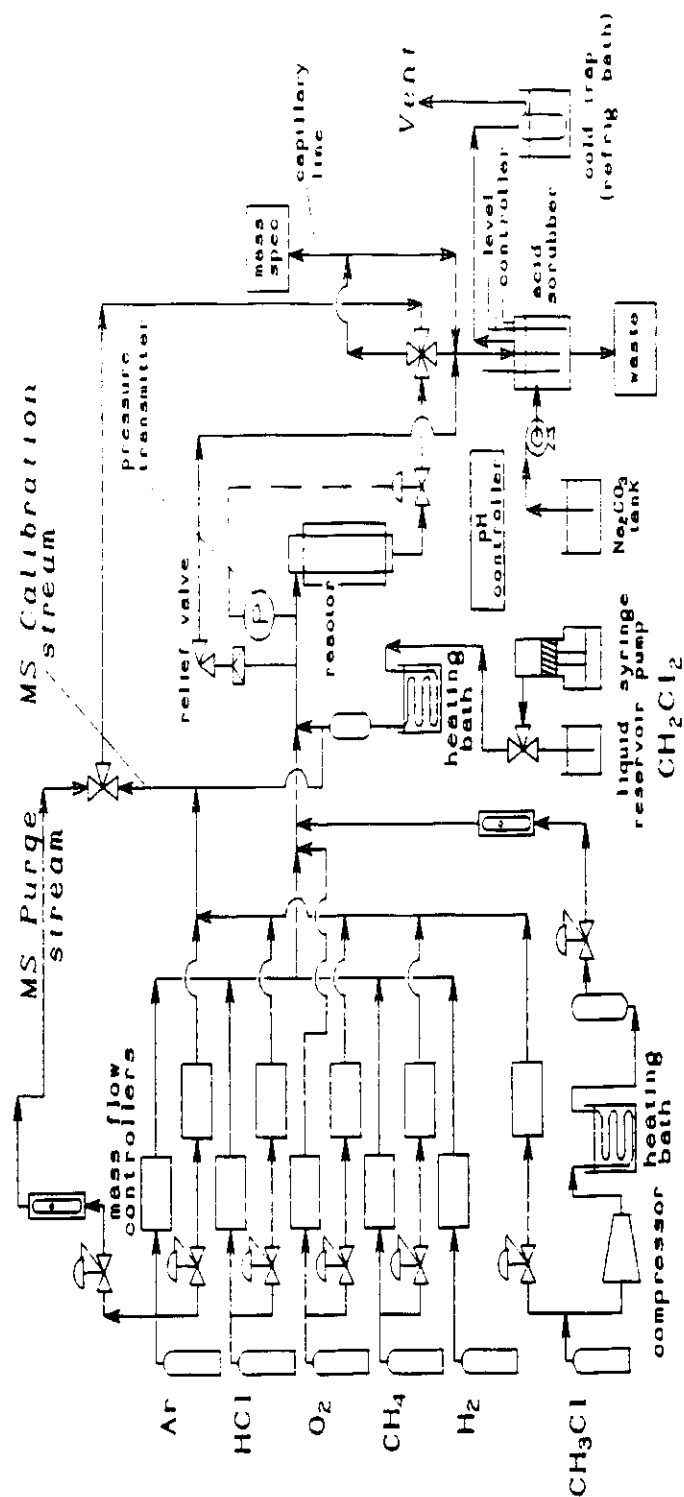


FIGURE 9. FLOW DIAGRAM FOR THE HIGH-PRESSURE METHANE CONVERSION REACTOR.



## PRODUCT CHARACTERIZATION

This portion of the research is concerned with characterization of products from oligomerization of chloromethane over zeolite. The chloromethane, produced in the first step of the process by oxyhydrochlorination of methane, is subsequently passed over a Mobil ZSM-5 catalyst in the second step to produce gasoline.

## EXPERIMENTAL

The ZSM-5 was obtained from Mobil Oil Corporation in the ammonium form with a silica-to-alumina ratio of 70:1. The ammonium form was converted to the acid form by calcining in air at 538°C for 16 hours. Reactions were conducted in a 0.5 X 7.0 inch quartz reactor contained in a split-tube furnace. Feeds were supplied from compressed gas cylinders and controlled by Brooks ratio mass flow controllers. The liquid condensate was collected in an ice bath during a 185 hour experiment while the reactor was operated at approximately 360°C employing chloromethane and nitrogen flows of 8.2 and 5.0 mL per minute respectively.

Separation of the liquid products was accomplished utilizing a 100 meter X 0.25 mm ID fused silica column coated with a 0.5 micron film of 100% methylpolysiloxane (Petrocol DH) and a helium carrier gas having an average linear velocity of 31 cm per second at 30°C. The column was temperature programmed from 30°C to 220°C at 1°C per minute. Retention indices were calculated by adding a mixture of n-alkane bracketing standards to the product and calculating the retention indices using the van den Dool and Kratz equation. Retention indices so calculated were compared to the retention indices of hundreds of gasoline-range hydrocarbons determined using identical chromatographic conditions. The identifications made in this manner were confirmed by combined GC-MS and/or GC-FTIR. GC-MS was performed using a HP 5988A system equipped and operated with the same chromatographic column and conditions as above. Further confirmation of these identifications was obtained by combined GC-FTIR using a Digilab FTS 65 GC/C 32 system equipped with a HP 5880 GC and the same column mentioned above utilizing identical chromatographic conditions. The GC-FTIR experiments were performed at Digilab in Cambridge, Massachusetts.

The low boiling, low molecular weight products that were not condensed in the ice bath were determined by directly sampling the reactor effluent product vapor, and analyzing it by gas chromatography using a 50 meter X 0.32 mm porous layer open tubular (PLOT) column containing Al<sub>2</sub>O<sub>3</sub>/KCl. The PLOT column was operated isothermally at 70°C for 8 minutes then programmed to 220°C at 8°C per minute using a helium carrier gas.

## RESULTS AND DISCUSSION

A heavily instrumented bench scale microreactor has been built and operated in PETC's Indirect Liquefaction Division since January 1990 to study the nature of the chloromethane/zeolite reaction. In a typical experiment, chloromethane conversion varies from 98.5% to 100%. Over 240 compounds have been analytically separated in the reaction mixture and individual compounds constituting about 90 weight percent of the products have been identified. The high resolution gas chromatographic profile of the liquid condensate is shown in Figure 10. Numbered chromatographic peaks are identified in Table IV along with the methods of identification and the gas chromatographic retention indices determined for the peaks in the sample and the authentic compounds.

The identifications in Figure 10 and Table IV are positive. The area percent data reported in Table IV is approximately equal to the weight percent of the compound in the liquid condensate. Unfortunately, the direct relationship between peak area percent and weight percent is not always true because in a few cases two or more compounds coelute and only one could be identified. Additionally, the flame ionization detector response for hydrocarbons is different than that for chlorinated hydrocarbons. On balance, the relationship between area percent and weight percent is approximately correct.

The liquid condensate did not contain significant amounts of the low boiling, low molecular weight products formed during the reaction. These compounds were determined in a separate experiment by sampling the reactor effluent immediately after exiting the reactor and analyzing them using on-line gas chromatography employing an alumina PLOT column. The resulting gas chromatographic profile appears in Figure 11. The numbered chromatographic peaks are in Table V. The peaks identified in Table V were identified by matching the retention times of sample peaks with those of authentic standard hydrocarbons, and by combined GC-MS. When this sample was obtained, the reactor was operated using substantially different conditions than utilized for the condensed liquid product shown in Figure 10. The reactor was operated at 350°C, 0.15 grams catalyst, and a total flow rate of 8.1 mL/min 97.4% helium and 2.6% chloromethane. This resulted in chloromethane conversion of 67%, however, the same hydrocarbon product slate was observed. The data presented in Table V is the weight percent of products containing six carbon atoms or less.

Detailed study of the reaction products can provide evidence of reaction pathways and mechanisms occurring in the zeolite. For example, although only a few weight percent of the products contain chlorine, a large portion of them are 2-chloroalkanes. The reaction also produces hydrogen chloride and terminal olefins. It is postulated that the 2-chloroalkanes are formed by Markovnikov addition of hydrogen chloride to the terminal olefins. The addition reaction may occur in the reactor or post reactor.

At 360°C, 1,2,4-trimethylbenzene is a major organic product formed in the reaction, and constitutes about 45 weight percent of the total liquid product. Electrophilic aromatic substitution of benzene, one of the reaction products, to form 1,2,4-trimethylbenzene may occur during the reaction. Polymethylation is favored because the ring becomes activated following addition of the first methyl group and because of the excess chloromethane present. Tetra- and penta-methylbenzenes are also found in the product but in substantially lower amounts. These larger molecules have difficulty diffusing out of the pores of the intracrystalline ZSM-5 network. Among the tetramethylbenzenes formed, the 1,2,4,5-isomer, which has a kinetic diameter of 6.1 Å, predominates over the larger but more thermodynamically favored tetramethylbenzene isomers. The polymethylbenzenes have high (>100) octane numbers.

The initial chemical reactions that occur in the chloromethane/zeolite reaction, if known, would provide considerable insight into the entire reaction process. One possibility is that  $\text{CH}_3\text{Cl}$  eliminates  $\text{HCl}$  and forms a carbenoid with an aluminum center. Carbenoids are known to form cyclopropane products with olefins. The presence of cyclopropane or its derivatives in the reaction mixture would support and would be consistent with the presence of carbenoid intermediates. Neither cyclopropane nor its derivatives have yet been found in the products of the chloromethane/zeolite reaction. A concerted effort will soon

TABLE IV

Peak #	Compound Name	Method of Identification			Estimated	
		GC-MS	FTIR	Measured R.I.	Known R.I.	Weight Percent
1	Chloromethane	x		332.92	332.92	0.002
2	2-Methylpropane	x		353.53	353.53	0.005
3	Butane	x		400.00	400.00	0.004
4	(E)-2-Butene	x		406.42	408.40	0.003
5	(Z)-2-Butene	x	x	418.18	416.44	0.003
6	Chloroethane	x		423.96	424.09	0.003
7	3-Methyl-1-butene	x		445.14	445.18	0.003
8	2-Methylbutane	x	x	465.18	465.11	0.060
9	1-Pentene	x		483.67	483.39	0.004
10	2-Chloropropane	x	x	490.72	491.40	0.012
11	2-Methyl-1-butene	x		493.79	493.58	0.009
12	Pentane	x	x	500.00	500.00	0.043
13	(E)-2-Pentene	x	x	505.09	504.91	0.027
14	(Z)-2-Pentene	x	x	510.30	510.35	0.014
15	2-Methyl-2-butene	x		514.38	513.84	0.028
16	1-Chloropropane	x		528.79	528.77	0.006
17	2-Chloro-2-methylpropane	x	x	530.66	530.04	0.146
18	Cyclopentane	x	x	554.24	554.13	0.022
19	2-Methylpentane	x	x	560.52	560.46	0.209
20	3-Methylpentane	x	x	577.32	577.22	0.093
21	2-Methyl-1-pentene	x		583.43	583.35	0.008
22	1-Hexene	x		584.79	584.67	0.005
23	2-Chlorobutane	x	x	598.87	598.38	0.030
24	Hexane	x	x	600.00	600.00	0.109
25	(E)-3-Hexene	x	x	601.03	601.42	0.014
26	(Z)-3-Hexene	x	x	602.28	602.19	0.037
27	(E)-2-Hexene	x	x	603.43	603.38	0.013
28	(Z)-2-Hexene	x		610.48	610.48	0.017
29	(E)-3-Methyl-2-pentene	x		615.42	615.32	0.080
30	Methylcyclopentane	x	x	620.67	620.81	0.296

TABLE IV

Peak #	Compound Name	Method of Identification		Estimated		
		GC-MS	FTIR	Measured R.I.	Known R.I.	Weight Percent
31	2,3-Dimethyl-2-butene	x		624.32	624.38	0.016
32	1-Methylcyclopentene, and Benzene	x	x	641.72	642.00	0.136
33	2-Chloro-2-methylbutane	x	x	647.89	647.88	0.911
34	Cyclohexane	x	x	651.09	651.14	0.016
35	2-Methylhexane	x	x	661.02	661.15	0.165
36	(E)-5-methyl-2-hexene	x		661.50	661.57	0.017
37	1,1-Dimethylcyclopentane	x		665.48	665.63	0.064
38	Cyclohexene	x	x	667.76	667.80	0.021
39	3-Methylhexane	x	x	670.56	670.60	0.162
40	cis-1,3-Dimethylcyclopentane	x	x	677.50	677.64	0.151
41	trans-1,3-Dimethylcyclopentane	x	x	680.73	680.98	0.144
42	trans-1,2-Dimethylcyclopentane	x	x	683.95	684.01	0.086
43	(E)-3-Heptene	x		697.72	697.50	0.073
44	Heptane	x	x	700.00	700.00	0.074
45	(Z)-3-Heptene	x		701.00	700.88	0.072
46	(E)-2-Heptene	x		703.99	703.99	0.017
47	(Z)-2-Heptene	x		710.92	710.93	0.015
48	Methylcyclohexane	x	x	716.41	716.54	0.090
49	1,1,3-Trimethylcyclopentane	x	x	719.35	719.32	0.071
50	Ethylcyclopentane	x	x	727.03	727.17	0.163
51	3-Methylcyclohexene	x		729.10	729.06	0.015
52	4-Methylcyclohexene	x		729.80	729.83	0.027
53	1 $\alpha$ ,2 $\beta$ ,4 $\alpha$ -Trimethylcyclopentane	x		735.35	735.37	0.071
54	Methylbenzene	x	x	748.65	749.00	2.452
55	2-Methylheptane	x	x	763.50	763.03	0.078
56	4-Methylheptane	x	x	764.38	764.57	0.044
57	2-Chloro-2-methylpentane	x	x	766.54		0.254
58	1 $\alpha$ ,2 $\alpha$ ,4 $\beta$ -Trimethylcyclopentane	x		768.44	768.82	0.020
59	3-Methylheptane	x	x	770.68	770.98	0.070
60	cis-1,3-Dimethylcyclohexane	x		771.77	771.54	0.031
61	trans-3-Ethyl-1-methylcyclopentane	x	x	783.61		0.154

TABLE IV

Peak #	Compound Name	Method of Identification			Estimated	
		GC-MS	FTIR	Measured R.I.	Known R.I.	Weight Percent
62	<i>cis</i> -3-Ethyl-1-methylcyclopentane	x	x	785.94		0.130
63	Ethylbenzene	x	x	844.50	844.74	1.473
64	1,3-Dimethylbenzene	x	x	853.85	853.38	8.789
65	1,4-Dimethylbenzene	x	x	854.85	854.75	4.847
66	2-Methyloctane	x		864.77	864.60	0.051
67	1,2-Dimethylbenzene	x	x	875.88	875.89	4.041
68	(1-Methylethyl)benzene	x		909.43	909.62	0.008
69	Propylbenzene	x		938.65	938.20	0.195
70	1-Ethyl-3-methylbenzene	x	x	946.60	946.91	2.419
71	1-Ethyl-4-methylbenzene	x		948.48	948.90	1.427
72	1,3,5-Trimethylbenzene	x	x	954.28	954.69	0.701
73	1-Ethyl-2-methylbenzene	x		963.29	963.66	0.154
74	1,2,4-Trimethylbenzene	x	x	980.80	978.78	45.343
75	(2-Methylpropyl)benzene	x		994.39	994.48	0.090
76	(1-Methylpropyl)benzene	x		996.50	996.78	0.070
77	1,2,3-Trimethylbenzene	x	x	1004.87	1005.04	0.382
78	1-Methyl-3-(1-methylethyl)benzene	x		1007.40	1007.84	0.076
79	1-Methyl-4-(1-methylethyl)benzene	x		1010.45	1010.90	0.072
80	2,3-Dihydro-1H-indene	x		1015.41	1015.61	0.086
81	1,3-Diethylbenzene	x	x	1034.43	1034.64	0.268
82	1-Methyl-3-propylbenzene	x		1037.02	1037.76	0.325
83	1,4-Diethylbenzene	x	x	1040.66	1040.69	0.393
84	Butylbenzene	x		1041.77	1042.19	0.070
85	1-Ethyl-3,5-dimethylbenzene	x		1044.03	1044.15	0.047
86	1-Methyl-2-propylbenzene	x		1052.22	1052.67	0.002
87	2-Ethyl-1,4-dimethylbenzene	x	x	1062.32	1063.12	0.122
88	4-Ethyl-1,3-dimethylbenzene	x		1063.94	1064.79	0.221
89	4-Ethyl-1,2-dimethylbenzene	x		1069.99	1070.74	1.094
90	1,2,4,5-Tetramethylbenzene	x	x	1102.07	1101.84	5.381
91	1,2,3,5-Tetramethylbenzene	x	x	1104.97	1104.26	0.717
92	2,3-Dihydro-5-methyl-1H-indene	x		1120.99	1122.37	0.537

TABLE IV

Peak #	Compound Name	Method of Identification			Estimated	
		GC-MS	FTIR	Measured R.I.	Known R.I.	Weight Percent
93	1,2,3,4-Tetramethylbenzene	x	x	1135.84		0.301
94	1,2,3,4-Tetrahydronaphthalene	x	x	1140.47	1140.85	0.120
95	Naphthalene	x		1160.26	1158.51	0.150
96	1,2,3,4-Tetrahydro-6-methylnaphthalene	x		1246.28	1246.78	0.226
97	Pentamethylbenzene	x	x	1265.42	1265.49	0.092
98	2-Methylnaphthalene	x	x	1270.79	1271.01	0.472
99	1-Methylnaphthalene	x		1285.68	1286.53	0.038
100	1,2,3,4-Tetrahydro-2,6-dimethylnaphthalene	x		1301.61	1301.47	0.146
101	1,2,3,4-Tetrahydro-2,7-dimethylnaphthalene	x		1302.75	1302.11	0.018
102	1,2,3,4-Tetrahydro-6-ethylnaphthalene	x		1339.38	1340.02	0.020
103	2,6-Dimethylnaphthalene	x	x	1381.93	1381.69	0.343
104	1,6-Dimethylnaphthalene	x	x	1383.86		0.487
105	1,5-Dimethylnaphthalene	x	x	1398.40		0.130
106	2,3,6-Trimethylnaphthalene	x	x	1509.73		0.051
Total Area of Identified Peaks						89.111
Average Absolute Deviation of Measured R.I. to Known R.I.						0.31

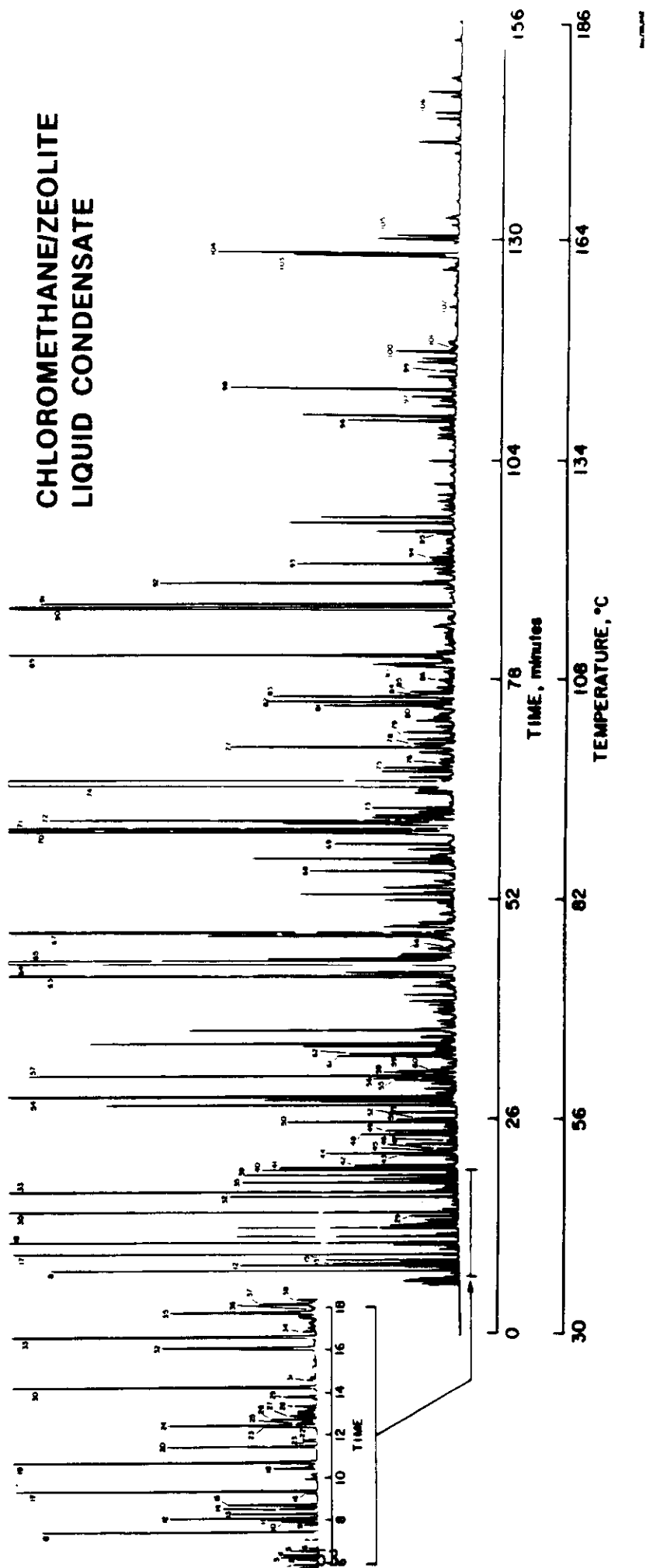


FIGURE 10. HIGH RESOLUTION GAS CHROMATOGRAPHIC PROFILE OF THE LIQUID CONDENSATE PRODUCT FROM THE CHLOROMETHANE REACTOR.

# CHLOROMETHANE/ZEOLITE REACTOR VAPORS ON $\text{Al}_2\text{O}_3$ PLOT COLUMN

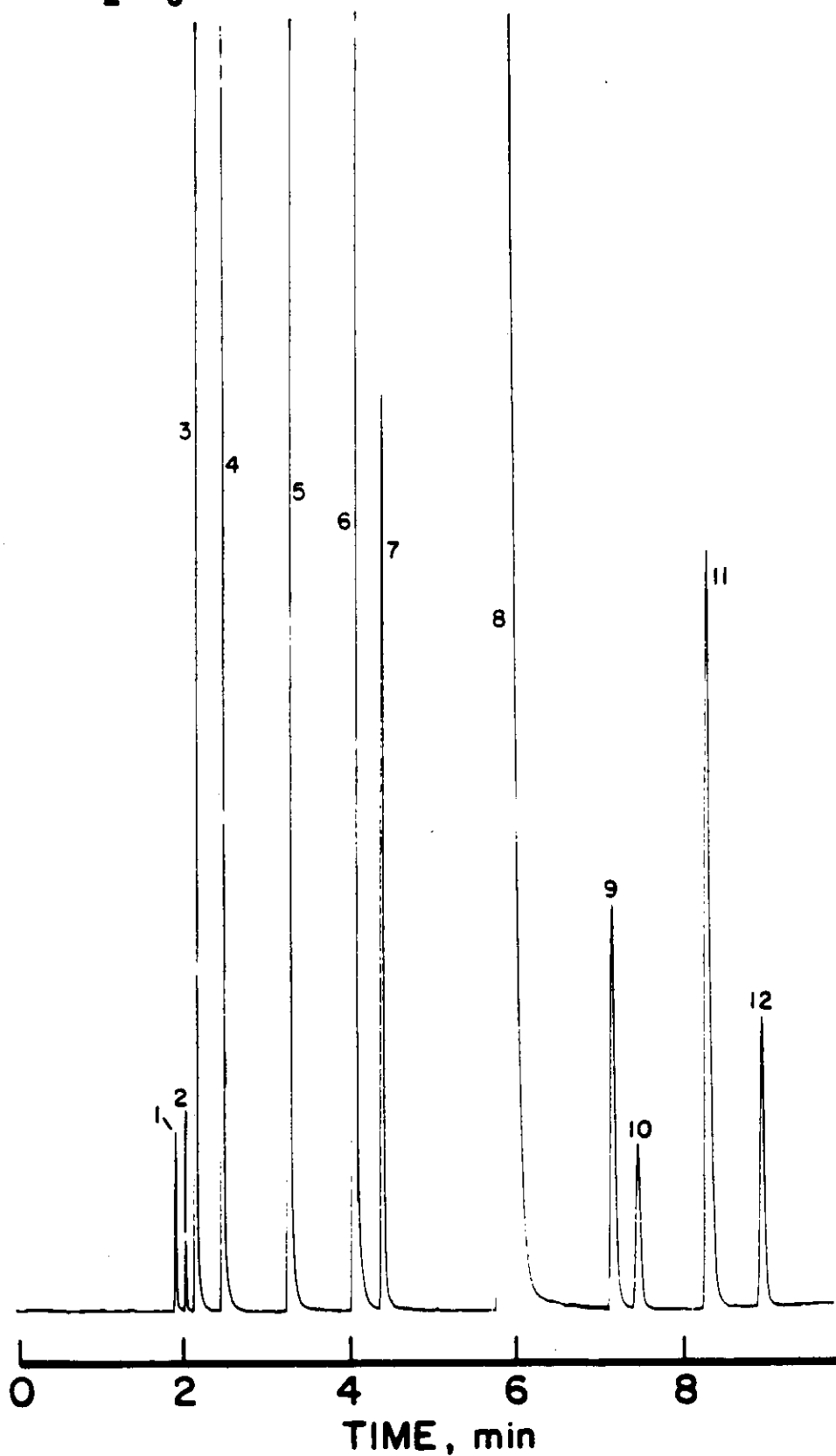


FIGURE 11. HIGH RESOLUTION GAS CHROMATOGRAPHIC PROFILE OF THE LOW-BOILING PRODUCT FROM THE CHLOROMETHANE REACTOR.



TABLE V

PEAK NUMBER	COMPOUND NAME	ESTIMATED WEIGHT % OF PRODUCTS CONTAINING SIX CARBON ATOMS OR LESS
1	Methane	0.51
2	Ethane	0.19
3	Ethene	8.22
4	Propane	11.4
5	Propene	20.5
6	2-Methylpropane	20.9
7	Butane	4.39
8	Chloromethane	-
9	(E)-2-Butene	3.63
10	1-Butene	1.51
11	2-Methylpropene	7.83
12	(Z)-2-Butene	2.40

begin to search for cyclopropane in products formed at low reaction temperatures and high space velocities. Detailed chemical analysis of the products formed during the chloromethane/zeolite reaction can provide considerable insight into the nature of intermediates, reaction mechanisms, and reaction pathways that occur in the zeolite's intracrystalline space, in turn suggesting ways to improve the process.

#### MECHANISM STUDIES

In an attempt to better understand the mechanism of the OHC reaction a micro-reactor was designed and constructed at PETC which is capable of operating at reaction conditions inside an electron paramagnetic resonance (EPR) spectrometer. The reactor has the ability to be operated at OHC reaction conditions while being contained inside of the EPR cavity.

#### EXPERIMENTAL

A sample of the Cu-OHC catalyst was placed in the micro-reactor (Figure 12) and placed inside the EPR cavity. The reactor was purged with nitrogen for 24 hours prior to the experiment. The temperature of the reactor was increased from room temperature to 300°C while spectra were collected at 50° intervals. The spectra were collected on a Varian model E-4 X-band spectrometer. Instrument settings were as follows: 100 KHz modulation frequency, 10 mW microwave power, modulation frequency of 9.379 GHz, field set 3355 G, and a scan range of 5000 G.

#### RESULTS AND DISCUSSION

A spectrum obtained at room temperature under a nitrogen purge (Figure 13) exhibited a broad  $\text{Cu}^{+2}$  band centered at approximately 3800 Gauss. As the temperature of the micro-reactor was increased the intensity of the band decreased until at 150°C all evidence of the band disappeared. Further investigation of this phenomena is planned along with observations while under activation of the catalyst and reaction conditions.

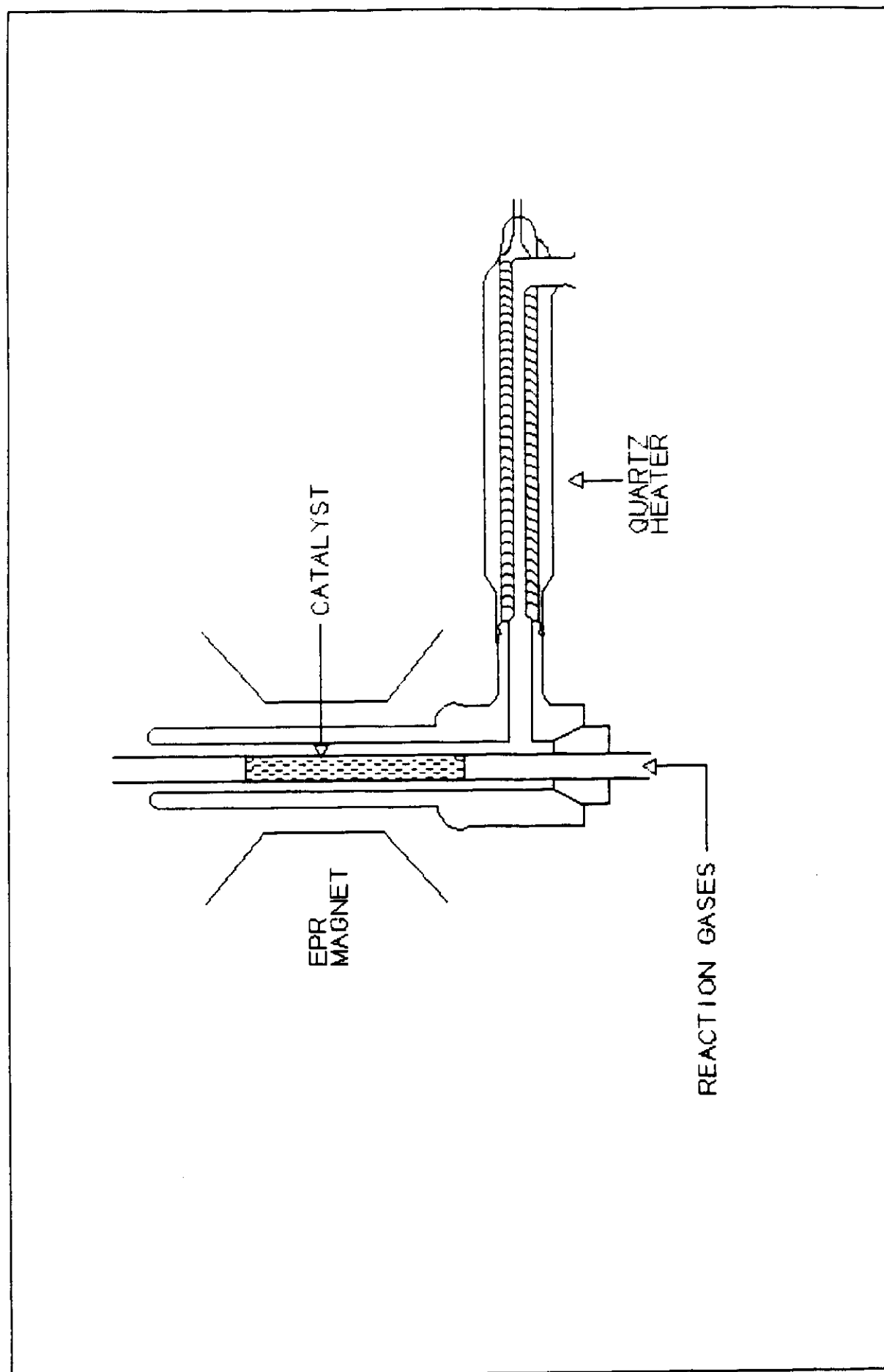


FIGURE 12. SCHEMATIC OF THE EPR MICRO-REACTOR.

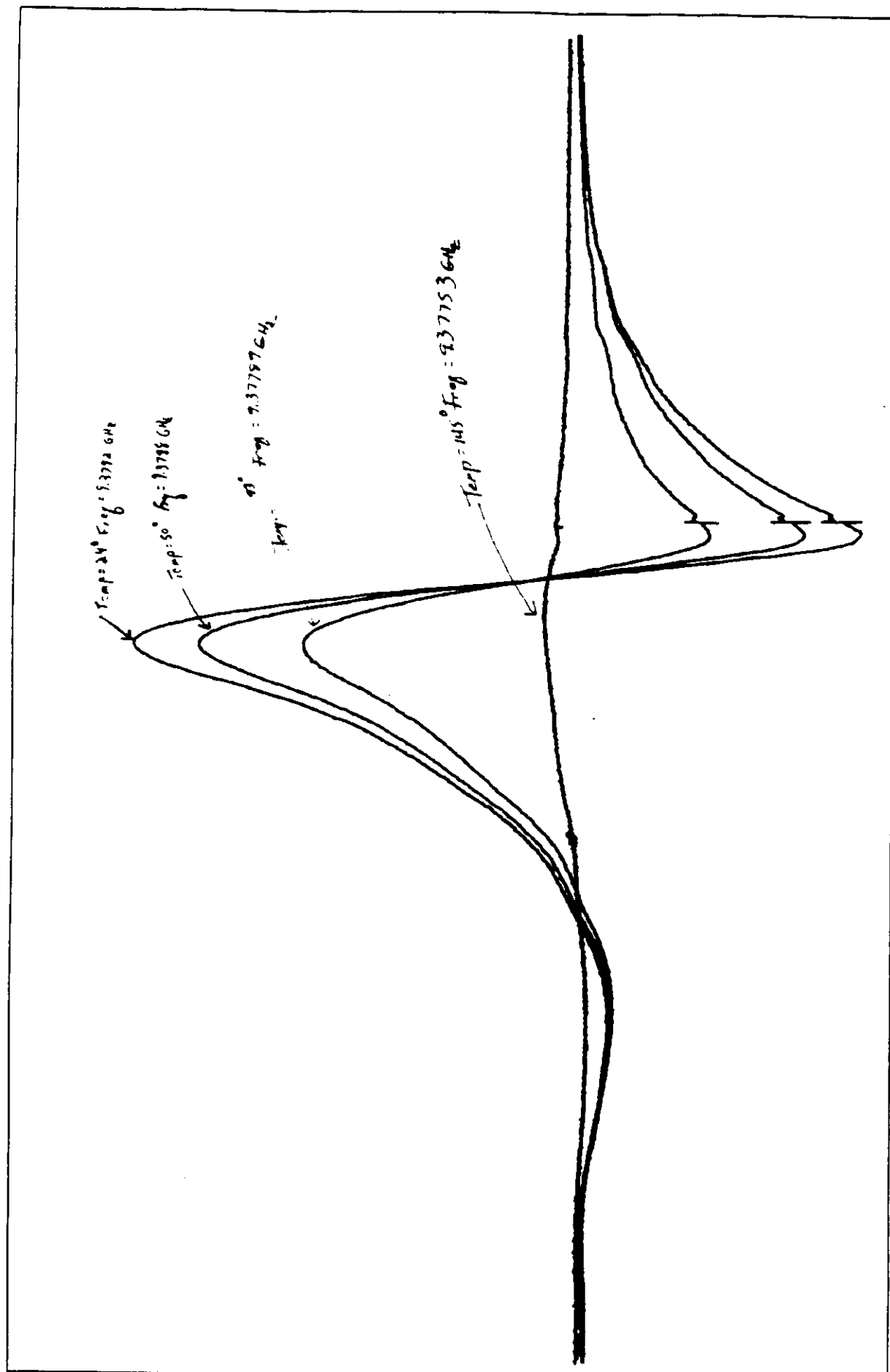


FIGURE 13. EPR SPECTRA OF THE VARIATION IN THE  $\text{Cu}^{2+}$  SIGNAL AS TEMPERATURE INCREASES FOR A FRESHLY PREPARED  $\text{Cu-OHC}$  CATALYST.

#### ACKNOWLEDGMENT

We would like to acknowledge the technical assistance of Joseph R. D'Este, Louise J. Douglas, Elizabeth A. Frommell, Joseph P. Hackett, Leonard J. Shaw, and Joseph P. Tamlia.

#### DISCLAIMER

Reference in this report to any specific commercial product, process, or service is to facilitate understanding and does not necessarily imply its endorsement or favoring by the United States Department of Energy.

#### REFERENCES

1. R.P. Noceti, C.E. Taylor. U.S. Patent 4,769,504, September 6, 1988.
2. C.E. Taylor, R.P. Noceti, Proceedings of the 9<sup>th</sup> International Congress on Catalysis, Vol. 2, 990, 1988.
3. J. M. Fox, T. P. Chen, and B. D. Degen. Chemical Engineering Progress, 86, 42 (1990).